Journal of Radiation Research, 2013, 54, 453–466
doi: 10.1093/jrr/rrs128 Advance Access Publication 7 January 2013

Nature of nontargeted radiation effects observed during fractionated irradiation-induced thymic lymphomagenesis in mice

Hideo TSUJI[1,*], Hiroko ISHII-OHBA[1], Tadahiro SHIOMI[1], Naoko SHIOMI[1], Takanori KATSUBE[1], Masahiko MORI[1], Mitsuru NENOI[1], Mizuki OHNO[2], Daisuke YOSHIMURA[3], Sugako OKA[4], Yusaku NAKABEPPU[4], Kouichi TATSUMI[1], Masahiro MUTO[1] and Toshihiko SADO[1]

[1]Research Center for Radiation Protection, National Institute of Radiological Sciences, 4-9-1 Anagawa, Inage-ku, Chiba 263-8555, Japan
[2]Department of Medical Biophysics and Radiation Biology, Faculty of Medical Science, Kyushu University, 3-1-1 Maidashi, Fukuoka 812-8582, Japan
[3]Department of Internal Medicine, Saiseikai Fukuoka General Hospital, 1-3-46 Tenjin, Chuoh-ku, Fukuoka 810-0001, Japan
[4]Division of Neurofunctional Genomics, Department of Immunobiology and Neuroscience, Medical Institute of Bioregulation, Kyushu University, 3-1-1 Maidashi, Fukuoka 812-8582, Japan
Corresponding author. Tel: +81-43-206-3165; Fax: +81-43-251-4268; E-mail: tsujihid@nirs.go.jp

(Received 13 June 2012; revised 28 November 2012; accepted 30 November 2012)

Changes in the thymic microenvironment lead to radiation-induced thymic lymphomagenesis, but the phenomena are not fully understood. Here we show that radiation-induced chromosomal instability and bystander effects occur in thymocytes and are involved in lymphomagenesis in C57BL/6 mice that have been irradiated four times with 1.8-Gy γ-rays. Reactive oxygen species (ROS) were generated in descendants of irradiated thymocytes during recovery from radiation-induced thymic atrophy. Concomitantly, descendants of irradiated thymocytes manifested DNA lesions as revealed by γ-H2AX foci, chromosomal instability, aneuploidy with trisomy 15 and bystander effects on chromosomal aberration induction in co-cultured ROS-sensitive mutant cells, suggesting that the delayed generation of ROS is a primary cause of these phenomena. Abolishing the bystander effect of post-irradiation thymocytes by superoxide dismutase and catalase supports ROS involvement. Chromosomal instability in thymocytes resulted in the generation of abnormal cell clones bearing trisomy 15 and aberrant karyotypes in the thymus. The emergence of thymic lymphomas from the thymocyte population containing abnormal cell clones indicated that clones with trisomy 15 and altered karyotypes were prelymphoma cells with the potential to develop into thymic lymphomas. The oncogene *Notch1* was rearranged after the prelymphoma cells were established. Thus, delayed nontargeted radiation effects drive thymic lymphomagenesis through the induction of characteristic changes in intrathymic immature T cells and the generation of prelymphoma cells.

Keywords: reactive oxygen species; chromosomal instability; bystander effect; trisomy 15; prelymphoma cell

INTRODUCTION

Radiation induces thymic lymphomas with nearly 100% incidence in some wild-type strains of mice, e.g. C57BL female mice, after four consecutive irradiations of 1.6-Gy X-rays at 4- to 8-day intervals [1]. The lymphomagenic potential of radiation is elicited by DNA injury to directly exposed cells and delayed effects through changes in the thymic microenvironment, leading to secondary cell damage as a consequence of tissue damage [2–5]. Lymphoma development from nonirradiated immature T cells in thymuses transplanted into irradiated mice indicates that microenvironmental changes are involved in lymphomagenesis [6, 7]. Similar microenvironmental effects induce leukaemia [8], and mammary [9] and muscle tumours [10]. Radiation-induced thymic atrophy [11–13], a characteristic

microenvironmental change, is associated with thymic lymphomagenesis based on the fact that lymphomagenesis is suppressed through restoration of the thymic cellularity by bone marrow transplantation [11, 13].

Radiation-induced genetic damage results from conditions and factors that cause a variety of responses conventionally associated with direct DNA damage. Phenomena induced by indirect radiation effects through microenvironmental changes, the nontargeted effects, include delayed chromosomal instability, bystander effects, mutation induction and reproductive death [2, 3, 14, 15]. Nontargeted effects *in vivo* [16–19] are suspected to be involved in radiation-induced carcinogenesis through mutations and karyotypic changes [2, 4, 20, 21]. Genotype-dependent chromosomal instability in mouse mammary epithelial cells is correlated with susceptibility to mammary tumours [18, 22, 23]. Susceptibility to leukaemia/lymphoma is not correlated with genomic instability after irradiation [24], however, and therefore the role of nontargeted effects in tumourigenesis requires simultaneous evaluation of both events in identical systems.

Radiation-induced thymic atrophy is thought to produce an inflammatory response, such as the activation of inflammatory-type genes, production of cytokines and reactive oxygen species (ROS) in the thymus, and an interaction between immature T cells and infiltrated activated macrophages and neutrophils [2, 3, 5, 25, 26]. Chromosomal instability *in vivo* is thought to be due to ROS generated by radiation-induced inflammation [2, 3, 26]. In fact, delayed chromosomal instability is associated with ROS-mediated processes [2, 27]. Oxidative metabolism and stress-inducible proteins are also implicated in the signalling process of bystander effects [2, 14, 15, 27]. Thus, the nontargeted effects might reflect inflammatory-type responses to radiation-induced stress and injury [14, 28]. Although descendants of irradiated thymocytes induce ROS *in vivo* [29], it is not known whether the ROS cause chromosomal instability in thymocytes or whether ROS-mediated chromosomal instability is related to thymic lymphomagenesis.

Thymic lymphomas develop through the emergence of prelymphoma cells and their conversion to overt lymphoma [11, 30, 31]. TL2-positive cells injected into thymuses induce thymic lymphomas and are therefore considered prelymphoma cells [30]. Although prelymphoma cells are characterized as $CD4^{-}CD8^{-}$ to $CD4^{+}CD8^{+}$ cells [30, 31], their detailed characteristics and the involvement of nontargeted effects in their formation are not known.

To clarify the mechanisms underlying lymphomagenesis, we examined abnormal events occurring during radiation-induced thymic lymphomagenesis. The nontargeted radiation effects occurred in the stage of prelymphoma cell generation under conditions that produced thymic lymphomas in almost 100% of C57BL/6 mice irradiated with 1.8 Gy four times at 1-week intervals. We show here that ROS-mediated nontargeted radiation effects contribute to thymic lymphomagenesis by inducing characteristic changes in immature T cells and generating prelymphoma cells.

MATERIALS AND METHODS

Irradiation and thymocyte preparation

All animals were handled according to our institutional guidelines. Female 5-week-old C57BL/6J mice were irradiated four times with 1.8 Gy ^{137}Cs γ-rays (RCS-50, Tokyo Shibaura, Japan) at 1-week intervals, which resulted in the development of thymic lymphomas in almost 100% of the mice [1]. Mice were maintained in a specific pathogen-free facility for 1 year to monitor thymic lymphomagenesis. To examine the thymocyte characteristics, thymocytes were isolated 0 (2 h) to 13 weeks after the final irradiation by mildly rubbing the thymus with frosted slide glass within 30 min after the thymuses were isolated and placed in Dulbecco's modified Eagle's medium (D-MEM) supplemented with 10% heat-inactivated foetal bovine serum at room temperature. The thymocytes were suspended in the medium at 4°C until use in the experiments.

ROS measurement

Immediately after isolation, the thymocytes (2.5×10^6 cells) were incubated in 2.5 ml of 5 μM freshly prepared 5-(and-6)-chloromethyl-2′, 7'-dichlorodihydrofluorescein diacetate, acetyl ester (CM-H_2DCFDA; Molecular Probes, Eugene, OR, USA) in phosphate-buffered saline (PBS) for 30 min at 37°C. After washing once with PBS, the cells were suspended in 2.5 ml PBS containing 5 μg/ml propidium iodide. Fluorescence intensity was analysed in 5×10^4 viable cells by FACSCalibur flow cytometry (BD Biosciences, Mountain View, CA, USA). Because ROS values fluctuated somewhat between experiments, values relative to those in five nonirradiated mice examined simultaneously are shown.

γ-H2AX foci

Immediately after isolation, the thymocytes (5×10^6 cells) were fixed with 4% paraformaldehyde in PBS, permeabilized with 0.5% Triton-X 100 in PBS for 20 min, and then blocked with 10% goat serum for 1 h at room temperature to eliminate nonspecific antibody binding. The thymocytes were treated with 250-fold diluted anti-γ-H2AX mouse monoclonal antibody (Millipore, Billerica, MA, USA) in A-buffer (20 mM Tris-HCl, pH 7.4, 137 mM NaCl, 0.1% Tween20 and 5% non-fat milk) for 2 h at 37°C, and then with 80-fold diluted tetramethylrhodamine B isothiocyanate-conjugated secondary antibody (Dako Cytomation, Glostrup, Denmark) in A-buffer for 1 h at 37°C. The thymocytes were washed with PBS three times, and then once with 0.5% Tween20 in PBS. The number of large γ-H2AX foci, not nascent small foci, was counted in 100 cells per sample

under fluorescence microscopy (AX70, Olympus, Tokyo, Japan).

Cell lines

The human colon cancer cell line HCT116 bearing a defective mismatch repair gene, *hMLH1* [32], was obtained from ATCC and stocked at –85°C immediately after receipt. *XRCC4*$^{-/-}$ cells were isolated from HCT116 cells by gene targeting of *XRCC4* loci [33]. Confirmation of the targeted loci by Southern blotting and western blotting, and the sensitivity to DNA damaging agents based on a cell survival assay have been described previously [33]. Mouse mutant cell lines, *Ogg1*$^{-/-}$ (OG7L line) cells with deficient repair of oxidized base lesions and *Mth1*$^{-/-}$ (T5 line) cells with deficient hydrolysis of oxidized nucleotides, were established from embryos of the respective mutant mice by long periods of *in vitro* culture, as described previously [34, 35]. *Mutyh*$^{-/-}$ mouse embryo fibroblasts lacking adenine/2-hydroxyadenine DNA glycosylase were isolated from embryos (13.5 days postcoital) obtained by mating *Mutyh*$^{+/-}$ mice ($n = 12$, C57BL/6J background), and maintained for 40 passages in D-MEM supplemented with 10% heat inactivated foetal bovine serum. Cells that spontaneously immortalized were designated as the *Mutyh*$^{-/-}$ (Y12L) line. The mutated loci in established cell lines were confirmed by genomic polymerase chain reaction (PCR) and western blotting, as described previously [34–36], and oxidative damage repair deficiency of the OG7L and Y12L lines was verified using a nicking assay, as described previously [34, 37]. Mth1 deficiency was verified using an 8-oxo-dGTPase assay, as described previously [35]. Once cell lines were established, the cells were stocked and used for experiments within 1 month after re-culture.

Chromosomal instability

To analyse chromosomal instability *in vivo* and *in vitro*, thymocytes (5×10^6 cells) were incubated with 100 ng/ml Colcemid in D-MEM for 3 h or cultured with 5 ml D-MEM for 48 h with 10 ng/ml phorbol 12-myristate 13-acetate (PMA; Sigma, St. Louis, MO, USA), 250 ng/ml ionomycin (Calbiochem, San Diego, CA, USA), and 50 μM 2-mercaptoethanol at 37°C in a humidified 5% CO_2 atmosphere, and treated with Colcemid for the last 1 h of the culture [38]. Chromosomes were prepared according to the air-drying method. Forty metaphase cells were observed for aneuploidy induction in each sample. Chromosomal aberrations were scored on coded slides in 200 cells per sample according to the ISCN (1995) criteria [39]. Translocations, inversions and interstitial deletions were omitted from the score due to ambiguity in non-banded chromosomes.

Bystander effects on chromosomal aberration induction

Post-irradiation thymocytes were co-cultured with ROS-sensitive or -insensitive human or mouse mutant cell lines and the induction of chromosomal aberrations in co-cultured mutant cells was examined. Two protocols were used; one was co-culture with proliferation stimuli in which thymocytes were viable for 48 h, but PMA induced chromosomal aberrations. The other was co-culture without the proliferation stimuli in which the thymocytes were not viable after 24 h, but there were no PMA-induced chromosomal aberrations. Thymocytes (5×10^6) were co-cultured with 10^5 *XRCC4*$^{-/-}$ cells for 48 h in D-MEM in the presence of PMA, ionomycin and 2-mercaptoethanol. In some experiments, 5×10^6 thymocytes were co-cultured with 10^5 *XRCC4*$^{-/-}$ cells or mouse *Mutyh*$^{-/-}$, *Ogg1*$^{-/-}$, or *Mth1*$^{-/-}$ cells for 24 h at 37°C without the proliferation stimuli in sodium pyruvate-free D-MEM with a high-concentration glucose (Invitrogen, Carlsbad, CA, USA) to avoid PMA-induced chromosomal aberrations and minimize the reduction of ROS in the medium. To examine the involvement of ROS in the bystander effect, the co-culture was incubated for 24 h with 2 U/ml Cu, Zn-superoxide dismutase (SOD: Wako Pure Chemical, Osaka, Japan) and 1.8 U/ml catalase (Wako). To examine the effect of immature T cells on bystander effects, 5×10^6 thymocytes were pretreated for 1 h with 0.3125 μg/ml anti-Thy1.2 antibody (Bay Bioscience, Kobe, Japan) at 4°C and then with 15-fold diluted rabbit anti-mouse complement (Cedarlane, Burlington, Canada) for 1 h at 37°C to kill the Thy1-2-positive cells. Treated thymocytes were co-cultured with 10^5 *XRCC4*$^{-/-}$ or *Mutyh*$^{-/-}$ cells for 24 h at 37°C. Chromosomal aberrations were scored in 100 metaphase cells per sample. The mean numbers of chromosomes in *XRCC4*$^{-/-}$, HCT116, *Mutyh*$^{-/-}$, *Ogg1*$^{-/-}$, and *Mth1*$^{-/-}$ cells were 45.3, 45.1, 74.3, 78.2 and 80, respectively. The frequency of chromosomal aberrations was calculated on a per cell basis.

H_2O_2 treatment

Nonirradiated thymocytes were cultured with the proliferation stimuli for 24 h at 37°C, treated with 0 to 200 μM H_2O_2 for 1 h, and then cultured with catalase for 31 h or 39 h in the presence of the proliferation stimuli to progress through one or two cell cycles. The induction of chromosomal aberrations or aneuploidy was examined in 100 first-cycle or second-cycle metaphases, respectively. To examine the induction of abnormal chromosome segregation by ROS, HCT116 cells grown on a chamber slide were treated with 0–20 μM H_2O_2 in PBS for 30 min at 37°C, washed and grown in the medium at 37°C for 4–6 h. The cells were fixed *in situ* with methanol-acetic acid (5:1, v:v) for 15 min and stained with Giemsa for 10 min. Abnormal

anaphase cells with chromatid bridges and/or lagging chromatids were examined in 50 to 100 cells at each post-treatment time. To examine the causal relationship between aneuploidy induction and the induction of chromatid bridges and lagging chromatids, HCT116 cells were grown for two cell cycles (22 h) after treatment with H_2O_2. Chromosomes were prepared after 1-h Colcemid treatment and counted in 100 metaphase cells.

Fluorescence in situ hybridization

Probes for chromosome 15 (Spectral Imaging, Tokyo, Japan) or chromosomes 1–7, 8–14 or 15–Y (Cambio, Cambridge, UK) were applied to the slides, denatured at 74°C for 4 to 8 min, and then incubated at 37°C for 18 h. The slides were washed and counterstained with DAPI in antifade reagent (Invitrogen) according to the manufacturer's instructions. To detect trisomy 15 or karyotypic changes, 50 metaphase cells were observed directly, or 10 to 50 metaphase cells were photographed using a CCD camera with IPLab software (Photometrics, Tucson, AZ, USA). The composite karyotype was constructed according to the ISCN (1995) [39].

Flow cytometry

Expression of Thy1.2 was analysed in 5×10^4 thymocytes treated with phycoerythrin-conjugated anti-Thy1.2 antibody (BD Biosciences) by FACSCalibur Flow Cytometry (BD Biosciences).

Notch1 rearrangement

Notch1 deletions in the whole locus were examined in thymic lymphomas by PCR as described previously [40, 41]. In thymocytes, only deletions at the 5'-end region between positions 4926 and 16 674 or between 8191 and 16 674 were detected [40]. Their frequencies were examined by nested PCR, as described previously [40].

Cell clonality

PCR was conducted with *TCRβ* primers, D1 in the diversity region and J1.6 in the joining region, or D2 and J2.6, or D1 and J2.6, and 0.5 μg DNA (equivalent to 10^5 cells) as described previously [42]. When the intensities of the recombination products in the electrophoresis gel were approximately equal to those in nonirradiated thymocytes, thymocytes were judged to be non-clonal. When one product was more intense than the other products, the thymocyte population was regarded as a partial clone. One product alone or several products observed without the background bands were regarded as mono-clones or oligo-clones, respectively. Germline bands were excluded from judgement. At least 10 mice were used to determine the percentage of clone-bearing thymuses at each post-irradiation week.

DNA sequencing

After electrophoresis, rearranged *Notch1* fragments and *TCRβ* recombinants were purified using a Gene CleanII kit (BIO 101, Carlsbad, CA, USA) and directly sequenced by the dye-termination method with a Prism 710 sequencer (Applied Biosystems, Foster, CA, USA).

Prelymphoma assay

C57BL/6 thymocytes (2×10^6 cells) isolated 6 to 10 weeks after irradiation were injected intrathymically in 3.79-Gy-irradiated C57BL/6 mice expressing enhanced green fluorescent protein (C57BL/6-EGFP) as described previously [30]. The recipient mice were pre-irradiated to facilitate the development of thymic lymphomas from the prelymphoma cells in the injected thymocytes. Mice were maintained for 1 year in a specific pathogen-free facility to monitor thymic lymphomas. The lymphoma origin was determined by the presence or absence of the *EGFP* gene by PCR. PCR was performed with primers, F1-2 (5'-TACAACTACAACAGC CACAACGTC-3') and R1-2 (5'-TCCAGCAGGACCATGT GATCGC-3'), 0.1 μg genomic DNA, and Ex Taq polymerase (Takara bio, Ohtu, Japan) for 28 cycles of 94°C for 30 s, 58°C for 30 s and 72°C for 2 min.

Statistical analysis

The difference between the mean value ± standard deviation in control nonirradiated mice and irradiated mice was statistically analysed using a *t*-test. A *P* value of less than 0.05 was considered statistically significant.

RESULTS

Radiation-induced thymic atrophy and ROS induction in thymocytes

Thymic cellularity in C57BL/6 mice was decreased for 6 weeks after four consecutive whole-body irradiations of 1.8-Gy γ-rays and then returned to just below normal levels at Week 8 (Fig. 1A). The proportion of Thy1.2-positive cells in the thymuses was slightly decreased, but still remained high during the stage with decreased thymic cellularity (Fig. 1B).

ROS production was monitored by incubating the thymocytes with CM-H_2DCFDA, which is stably retained in the cells and fluoresces after oxidation. ROS levels increased by Week 2 in post-irradiation thymocytes, and further increased after 8 weeks (Fig. 1C). The decrease in ROS levels at 0 weeks (2 h after irradiation) might represent a weak reaction of cells attempting to convert the CM-H_2DCFDA to a fluorescent material as a consequence of direct radiation insult.

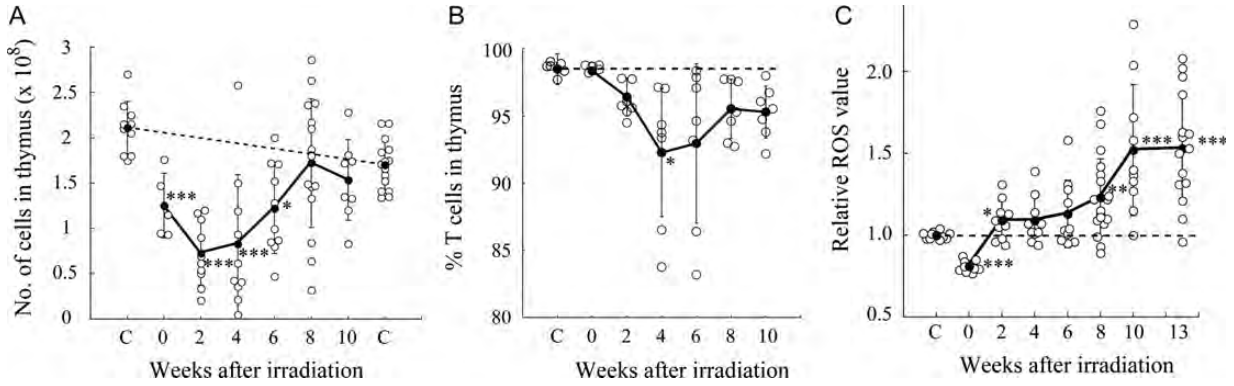

Fig. 1. Radiation-induced thymic atrophy and ROS induction in post-irradiation thymocytes. Open circles and closed circles with bars indicate individual mouse data and mean values ± standard deviations, respectively. Asterisks indicate significant differences in mean values between control and irradiated mice [*t*-test, $P < 0.05$ (*), 0.01 (**) and 0.001 (***)]. Broken lines indicate baseline levels. (**A**) Thymic cellularity after split-dose irradiations. The left and right 'C's show values in 8- and 18-week-old nonirradiated mice, respectively. (**B**) Percentage of Thy1.2-positive cells in thymuses after irradiation. (**C**) Induction of ROS in post-irradiation thymocytes. ROS values relative to those in control thymocytes are shown.

Induction of DNA lesions and chromosomal instability in post-irradiation thymocytes

The delayed ROS production suggested that thymocytes accumulated ROS-mediated DNA damage, so we examined the induction of γ-H2AX foci, as a marker of DNA lesions (Fig. 2A). The number of γ-H2AX foci increased immediately (2 h) after irradiation, due to radiation-induced direct DNA damage and then decreased to baseline by Week 4. At 6 to 13 weeks after irradiation, the foci levels were significantly increased. Thus, the induction of DNA lesions was coincident with the induction of ROS in post-irradiation thymocytes.

Delayed induction of ROS and DNA lesions suggested that chromosomal instability could be induced in post-irradiation thymocytes. We examined numerical and structural chromosomal abnormalities in thymocytes after *in vitro* culture for 48 h with PMA, ionomycin and 2-mercaptoethanol. Aneuploidy was significantly induced, based on the mean aneuploidy, in post-irradiation thymocytes, while the frequencies were widely distributed (Fig. 2B). Aneuploidy was also observed in the majority of thymic lymphomas. Most aneuploid thymocytes and thymic lymphomas contained 41 chromosomes (see Supplementary Table 1).

To confirm that aneuploidy was an intrinsic characteristic of post-irradiation thymocytes, and not a PMA-induced artefact, the chromosome number was compared between thymocytes incubated with Colcemid for 3 h and thymocytes cultured with PMA, ionomycin and 2-mercaptoethanol for 48 h. Percentage aneuploidy in post-irradiation thymocytes prepared from eight mice was exactly the same between the two conditions (see Supplementary Table 2), indicating that aneuploidy was an intrinsic characteristic of post-irradiation thymocytes. Aneuploidy occurred in immature T cells because most post-irradiation thymocytes were Thy1.2-positive (c.f. Fig. 1B).

To examine the causal relationship between ROS induction and aneuploidy induction, nonirradiated thymocytes were treated with H_2O_2 in medium for 1 h, and cultured for two cell cycles (Fig. 2C). H_2O_2 induced aneuploidy in a dose-dependent manner, suggesting that the ROS induced aneuploidy in thymocytes. The possibility was strengthened by the fact that H_2O_2 induced lagging chromatids and chromatid bridges at anaphase in the first cell cycle in HCT116 cells (see Supplementary Fig. 1A and B), which was followed by an increase in the proportion of aneuploid cells in the second cell cycle (see Supplementary Fig. 1C).

Aneuploid thymocytes bear trisomy 15 [38] and thus trisomy 15 in thymocytes was examined by chromosome 15 painting (Fig. 2D and Table 1). The percentage of trisomy 15 was similar to the percentage of aneuploidy, suggesting that most aneuploid cells contained trisomy 15.

Delayed structural chromosomal abnormalities were also induced in post-irradiation thymocytes cultured with proliferation stimuli (Fig. 2E and F). The frequent chromosomal aberrations observed at 0 weeks (2 h) were due to direct radiation damage. The majority of aberrations 6 to 13 weeks after irradiation were chromatid-type aberrations (see Supplementary Table 3), indicating that aberrations were generated during the ongoing cell cycle.

PMA is a potent inducer of chromosomal aberrations [43], so it is uncertain whether the chromosomal aberrations observed in thymocytes cultured with PMA were due to chromosomal instability or to the PMA. We examined aberration frequencies in thymocytes incubated with Colcemid for 3 h in the absence of the proliferation stimuli. Aberrations were induced at a significantly higher frequency in post-irradiation thymocytes than in similarly

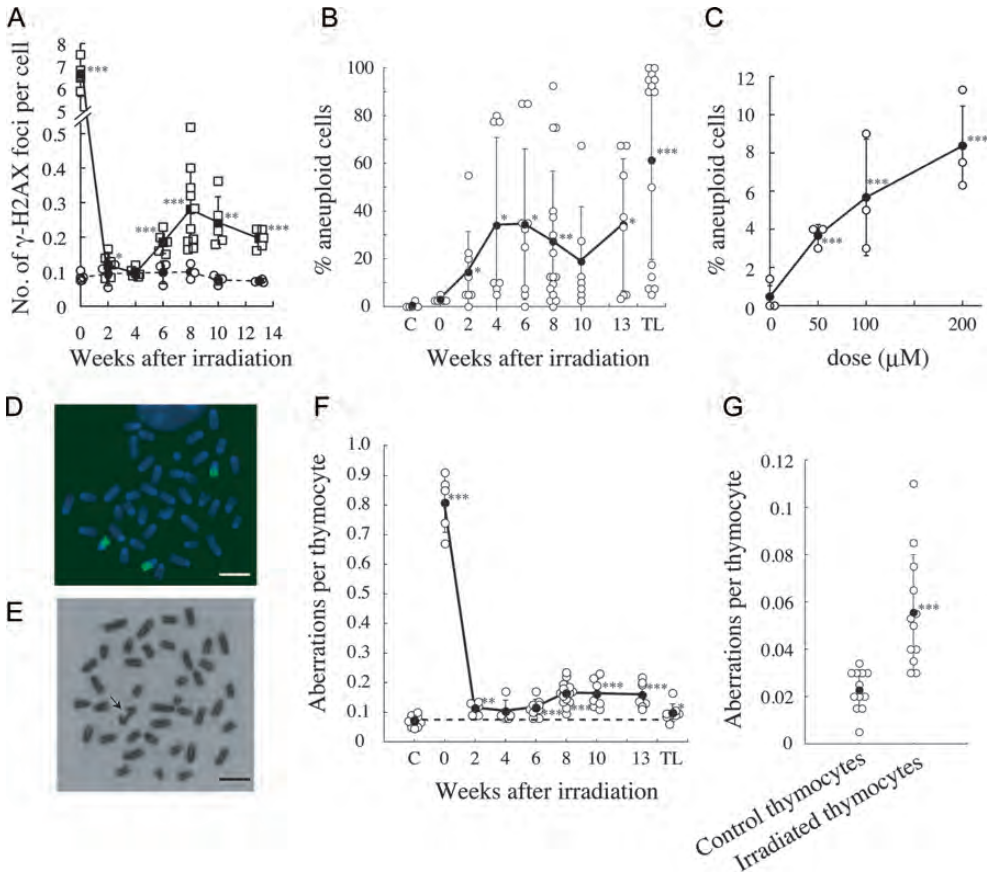

Fig. 2. Delayed induction of γ-H2AX foci and chromosomal instability in post-irradiation thymocytes. Symbols are the same as those in Fig. 1 except that in (A), open squares and closed squares indicate individual irradiated mouse data and mean values ± standard deviations, respectively. Open circles and closed circles indicate individual control mouse data and mean values ± standard deviations, respectively. TL, thymic lymphoma. (**A**) Delayed induction of γ-H2AX foci after irradiation. (**B**) Delayed appearance of aneuploidy after irradiation. (**C**) Induction of aneuploidy by H_2O_2 in thymocytes. (**D**) Trisomy 15 in a thymocyte 8 weeks after irradiation. Bar, 10 μm. (**E**) Chromatid break (arrow) in a thymocyte 8 weeks after irradiation. Bar, 10 μm. (**F**) Delayed induction of chromosomal aberrations in post-irradiation thymocytes cultured with proliferative stimuli for 48 h. (**G**) Induction of chromosomal aberrations *in vivo* in thymocytes 8 weeks after irradiation.

treated nonirradiated thymocytes (Fig. 2G). Thus, delayed chromosomal instability was an *in vivo* characteristic of post-irradiation thymocytes.

To clarify the involvement of ROS in structural chromosomal abnormalities, nonirradiated thymocytes were treated with 50–200 μM H_2O_2 and grown for one cell cycle. H_2O_2 induced chromosomal aberrations in a dose-dependent manner (see Supplementary Fig. 2), supporting the causal relationship between ROS and chromosomal instability.

Bystander effects of post-irradiation thymocytes on chromosomal instability

The delayed chromosomal instability suggested that post-irradiation thymocytes produced clastogenic factors. To examine the bystander effects of such factors on the induction of chromosomal aberrations, DNA double-strand break repair-deficient and H_2O_2-sensitive human *XRCC4*$^{-/-}$ cells were co-cultured with post-irradiation thymocytes with proliferation stimuli. While co-culture with nonirradiated thymocytes had no effect, co-culture with thymocytes prepared immediately after irradiation (2 h) had a significant effect (Fig. 3A), possibly due to some clastogenic factors generated by direct radiation effects. Bystander effects were delayed in post-irradiation thymocytes 4 to 13 weeks after irradiation.

To examine whether the bystander effect was induced by ROS or ROS-reacted products, *XRCC4*$^{-/-}$ cells or *Mutyh*$^{-/-}$ cells with deficient repair of oxidized base lesions were co-cultured with thymocytes for 24 h in the presence of SOD and catalase, but without proliferation stimuli (Fig. 3B and C). Post-irradiation thymocytes induced chromosomal aberrations in both cell lines, indicating that

Table 1. Characterization of thymocytes injected intrathymically and resultant thymic lymphomas

Mice	Characteristics of injected thymocytes					No. of TLs/ No. of mice injected[d]	Characteristics of resultant thymic lymphomas			
	Presence of clones	*TCRβ* rearrangement[a]	% aneuploidy (% trisomy 15)	Karyotype[b]	*Notch1* rearrangement (fold)[c]		*TCRβ* rearrangement	Aneuploidy (trisomy15)[e]	Karyotype	*Notch1* rearrangement[e]
8w-14	Oligo	D2/J2.3, D2/J2.5	75 (87)	40, −X, +15, der(3)t(3;6), der(6)t(6;18), der(12)t(12;16), der(18)t(3;18)[3/14]	1	4/4	the same as thymocyte	1/4 (3/3)	conserved	4/4
8w-17	Oligo	D1/J1.4, D2/J2.2, D2/J2.7	75 (76)	41, del(X), +der(X)t(X;15)[9/10]	2	4/4	the same as thymocyte	4/4 (3/3)	conserved	4/4
8w-13	Partial	D1/J1.4, D2/J2.3	38 (44)	ND	13	4/5	the same as thymocyte	2/2 (2/2)	ND	2/3
6w-9	Partial	D1/J1.1, D2/J2.4	35 (23)	ND	2	5/5	the same as thymocyte	4/4 (3/3)	ND	4/5
10w-7	Partial	D1/J1.3	8 (8)	40, i(15), t(1;12)[2/34]	1	4/4	the same as thymocyte	4/4 (3/3)	conserved	2/4
8w-16	Partial	D1/J1.1, D2/J2.4	23 (16)	ND	1	5/6	the same as thymocyte	1/5 (0/3)	ND	3/5
10w-3	Oligo	D1/J1.4, D2/J2.3, D2/J2.5	68 (43)	ND	2	4/5	D2/J2.5	0/4 (0/2)	ND	4/4
10w-1	?	germline sequence	28 (38)	41, +15, t(2;12)[1/35]	1	4/5	–	2/4 (2/2)	conserved	4/4
6w-10	?	germline sequence	8 (4)	ND	3	3/5	–	3/3 (3/3)	ND	3/3
10w-4	–	–	13 (4)	ND	1	1/4	–	1/1 (1/1)	ND	1/1
6w-7	–	–	33 (ND)	ND	3	1/6	–	0/1 (0/1)	ND	1/1
8w-15	–	–	13 (ND)	ND	1	0/4				
10w-2	–	–	5 (0)	ND	2	0/4				

Continued

Table 1. *Continued*

Mice	Characteristics of injected thymocytes					No. of TLs/ No. of mice injected[d]	Characteristics of resultant thymic lymphomas			
	Presence of clones	*TCRβ* rearrangement[a]	% aneuploidy (% trisomy 15)	Karyotype[b]	*Notch1* rearrangement (fold)[c]		*TCRβ* rearrangement	Aneuploidy (trisomy15)[e]	Karyotype	*Notch1* rearrangement[e]
10w-5	–	–	10 (0)	ND	1	0/5				
10w-6	–	–	3 (0)	ND	1	0/5				
6w-8	–	–	0 (4)	ND	1	3/5	D2/J2.1, D2/J2.3	0/3 (0/1)	ND	3/3

[a]The minus (–) symbol indicates similar profiles of *TCRβ* rearrangements between irradiated and nonirradiated mice. Others indicate clones with rearrangements between the designated regions.

[b]Karyotype is shown in order of chromosome number, loss or gain of chromosomes, derivative chromosomes and the number of cells with the indicated karyotype/the number of cells examined. The derivative chromosomes with a plus symbol indicate the addition of derivative chromosomes accompanied by two normal chromosomes and those with no sign indicate the substitution of one normal chromosome with the derivative chromosome.

[c]*Notch1* rearrangements occurring between the hotspots are shown as fold increase compared with those in nonirradiated mice. Thymocytes bearing rearrangements at over 10-fold frequency existed as clones.

[d]Thymocytes (2×10^6 cells) 6–10 weeks after irradiation were injected intrathymically in 3.79-Gy-irradiated $EGFP^+$ mice. Origin of thymic lymphomas (TL) was determined by examining the presence or absence of the *EGFP* gene by PCR.

[e]Aneuploidy, trisomy 15 and *Notch1* rearrangements are shown as the number of lymphomas with indicated events/the number of lymphomas examined. *Notch1* was rearranged between the hotspots at the 5'-end region in lymphomas except that three rearrangements in 8w-16 and 6w-10 lymphomas occurred at the juxtamembrane extracellular domain.

ND, not done.

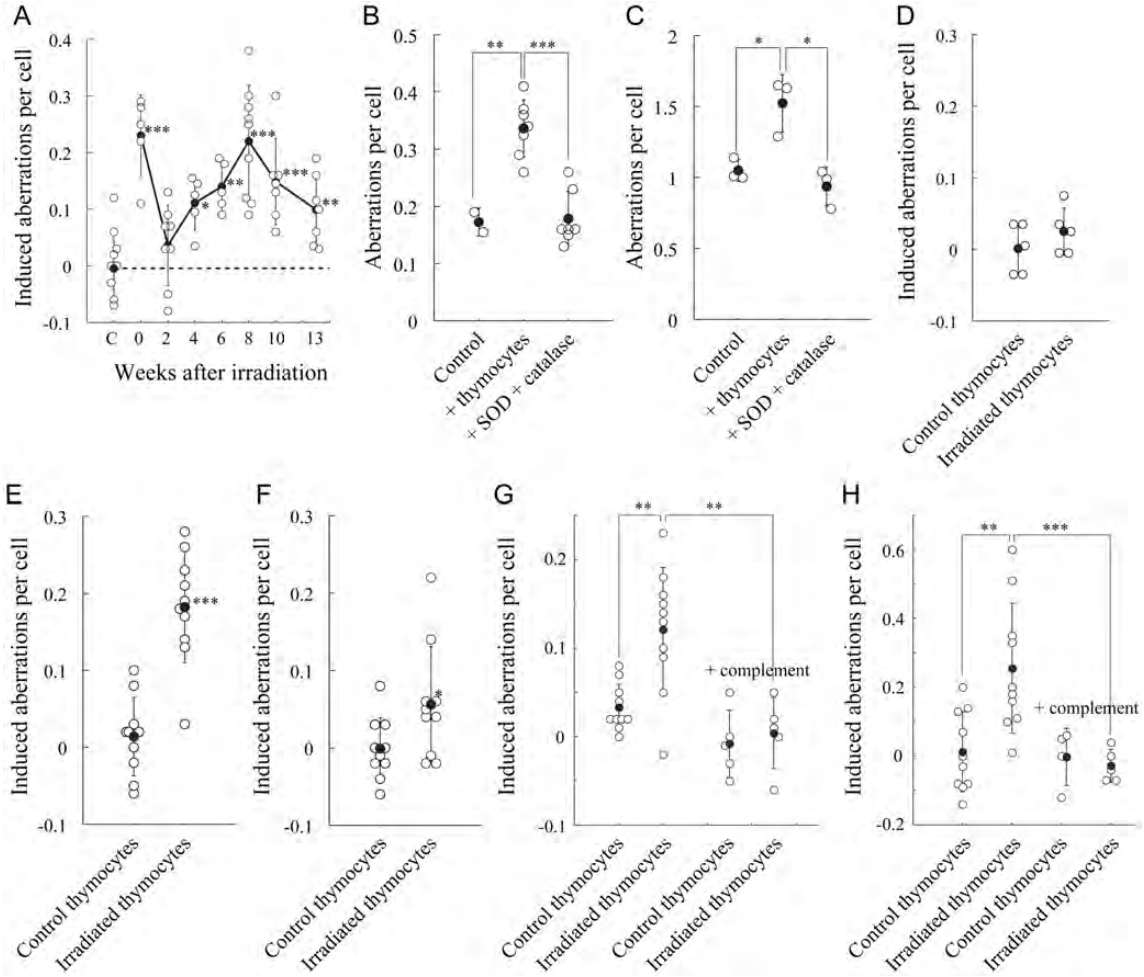

Fig. 3. Delayed induction of bystander effects in cells co-cultured with post-irradiation thymocytes. Symbols are the same as those in Fig. 1. (**A**) Bystander effect of post-irradiation thymocytes on chromosomal aberration induction in co-cultured *XRCC4*$^{-/-}$ cells. Aberrations are indicated as net increases. 'C' indicates the values in *XRCC4*$^{-/-}$ cells co-cultured with nonirradiated thymocytes. (**B** and **C**), Abolishment of bystander effects of post-irradiation thymocytes by SOD and catalase in co-cultured *XRCC4*$^{-/-}$ (B) or *Mutyh*$^{-/-}$ cells (C). Mutant cells were cultured without thymocytes (Control), with post-irradiation thymocytes 13 weeks after irradiation (+ thymocytes) or with post-irradiation thymocytes in the presence of SOD plus catalase (+ SOD + catalase) for 24 h. (D–F), Bystander effects of post-irradiation thymocytes in HCT116 (**D**), *OGG1*$^{-/-}$ (**E**) and *Mth1*$^{-/-}$ cells (**F**). Cells were co-cultured with control thymocytes or post-irradiation thymocytes at Week 8 for 24 h. (**G** and **H**) Abolishment of the bystander effect of post-irradiation thymocytes by complement treatment in *XRCC4*$^{-/-}$ (G) and *Mutyh*$^{-/-}$ cells (H). The cells were co-cultured with control thymocytes or post-irradiation thymocytes at Week 10. Thymocytes were pre-treated with anti-Thy1.2 antibody and complements (+ complement).

the bystander effect was an intrinsic characteristic. Treatment with SOD and catalase significantly decreased the aberration frequency in both cell lines, suggesting that the bystander effect was due to ROS or their reacted products.

We then examined whether the bystander effect of post-irradiation thymocytes was detectable in other cell lines and whether the bystander effect was attributable to immature T cells or other cell types in the thymus. Chromosomal aberrations were significantly induced in co-cultured *Ogg1*$^{-/-}$ cells with deficient repair of oxidized base lesions (Fig. 3E) and *Mth1*$^{-/-}$ cells with deficient hydrolysis of oxidized nucleotides (Fig. 3F), but not in mismatch repair-deficient HCT116 cells (Fig. 3D). When immature T cells were depleted by pre-treatment with anti-thy1.2 antibody and complements, bystander effects of thymocytes were abolished in co-cultured *XRCC4*$^{-/-}$ cells (Fig. 3G) and *Mutyh*$^{-/-}$ cells (Fig. 3H), indicating that the bystander effects were due to immature T cells.

Notch1 rearrangements

Thymic lymphomagenesis is accompanied by the activation of *Notch1* by rearrangements [41, 44] or mutations. We therefore examined intragenic *Notch1* deletions between

hotspots using nested PCR. Radiation-induced deletions were detected in some mice at 10- to 100-fold frequencies compared with background (Fig. 4). Those sequences were identical (see Supplementary Table 4), suggesting that cells with identical deletions expanded clonally.

Appearance of clones and generation of prelymphoma cells

The appearance of thymocytes bearing trisomy 15 or *Notch1* rearrangements suggested that abnormal clones emerged in the thymocyte population after irradiation. To more clearly demonstrate clonality, we conducted PCR of the *TCRβ* locus in post-irradiation thymocytes (Fig. 5A). All the recombination products were observed with similar intensities among nonirradiated mice and mice immediately after irradiation (0 weeks; Fig. 5B). In contrast, intensities of some products observed 2 to 10 weeks after irradiation were stronger than those in nonirradiated mice. Sequencing of typical intense bands revealed that one rearranged sequence was predominant in each individual (see Supplementary Table 5), suggesting that cells bearing a particular rearrangement expanded clonally. We divided the thymuses into non-clones, partial clones, oligo-clones and mono-clones. Post-irradiation thymocytes displayed clonality (Fig. 5C); partial clones were predominant in the early weeks of post-irradiation, and oligo-clones and mono-clones increased in later weeks.

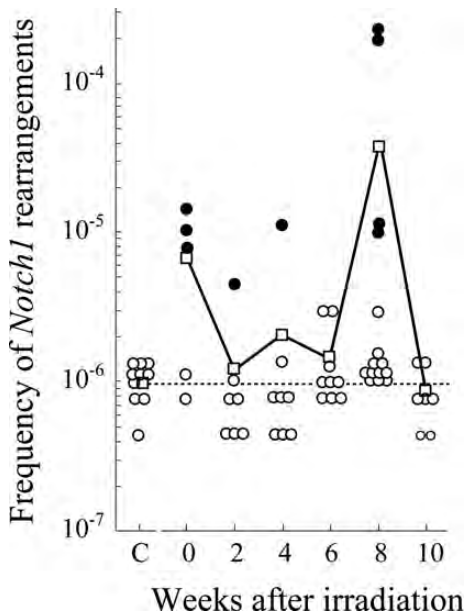

Fig. 4. Induction of intragenic deletions in *Notch1* gene after irradiation. Dotted lines, circles, closed circles, and squares indicate the background frequency, individual mouse data, clones with identical rearrangements and mean deletion frequencies, respectively.

To determine whether these clones were prelymphoma cells, we injected post-irradiation thymocytes into the thymuses of irradiated mice to assess lymphoma development. All *TCRβ* rearrangements in the resultant thymic lymphomas were identified as derivatives of those of the injected thymocytes (Fig. 5D).

The identification of prelymphoma cells, characteristics of injected thymocytes and resultant thymic lymphomas are summarized in Table 1. Thymic lymphomas developed from injected post-irradiation thymocytes, indicating that the injected thymocytes contained prelymphoma cells. All thymocyte populations bearing clones had a strong ability to develop thymic lymphomas. Sequencing revealed that the *TCRβ* rearrangements in the resultant lymphomas were identical to those in the injected thymocytes (see Supplementary Table 5), indicating that thymic lymphomas derived from the clones. Thus, most of the clones contained prelymphoma cells except for 10w-3 clones bearing rearrangements between D1 and J1.4 or between D2 and J2.3. Thymic lymphomas derived from 10w-1 and 6w-10 thymocytes possessed the germline *TCRβ* sequence. We did not judge the clonality of clones with the germline sequence. Six of seven other thymocyte populations without clones had only weak ability to develop into lymphomas (10w-4 and 6w-7) or did not contain prelymphoma cells (8w-15, 10w-2, 10w-5 and 10w-6). Only one population without clones (6w-8) contained prelymphoma cells that developed into lymphomas bearing *TCRβ* rearrangements. Because the *TCRβ* rearrangement sequences were identical among 6w-8 lymphomas (see Supplementary Table 5), prelymphoma cell clones with identical *TCRβ* rearrangements were judged to exist in the thymocyte population, but could not be detected as a clone due to the small number.

Six of seven (86%) of the thymocyte populations with clones had high frequencies of trisomy 15 and resultant thymic lymphomas also possessed trisomy 15, except for 8w-16 and 10w-3 lymphomas. In contrast, none of the thymocyte populations without clones (10w-4, 10w-2, 10w-5, 10w-6 and 6w-8) exhibited trisomy 15, while 33% (1/3) of their thymic lymphomas showed trisomy 15. In addition, none of the three thymocyte populations bearing no prelymphoma cells (10w-2 10w-5 and 10w-6) possessed trisomy 15. These findings suggested that the acquisition of trisomy 15 contributed to thymic lymphomagenesis, although there were other pathways in which trisomy 15 was not involved or trisomy 15 was acquired after prelymphoma cells were established.

All four thymocyte populations examined showed karyotypic changes. Identical alterations were conserved in the resultant thymic lymphomas (see Supplementary Fig. 2), indicating that cells bearing the specific karyotypes were prelymphoma cells. The frequency of thymocytes bearing the specific karyotype was relatively high in thymocyte populations containing oligo-clones, e.g. 3 of 14 cells in

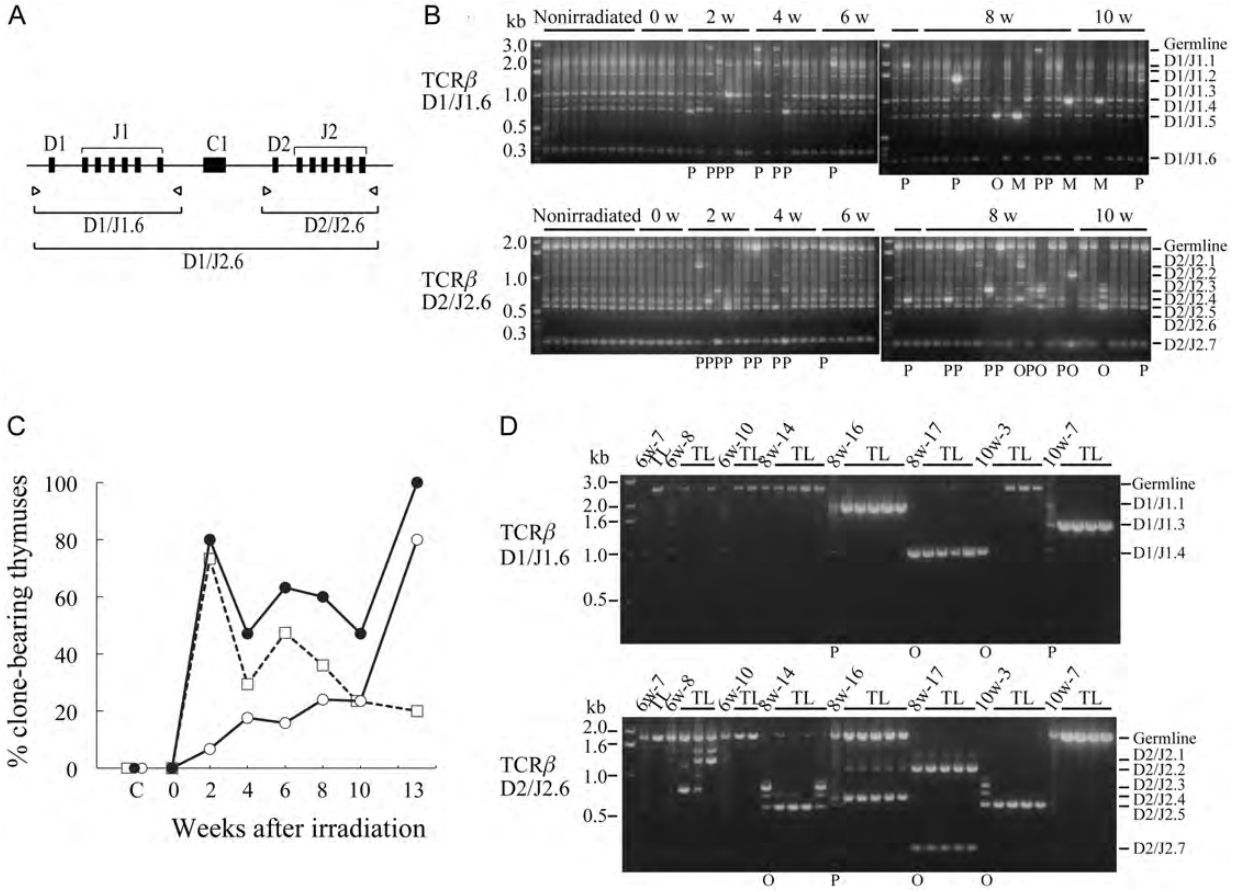

Fig. 5. Clonality revealed by *TCRβ* recombination. (**A**) Primer pairs used for PCR. (**B**) Examples of electrophoresis patterns of *TCRβ* recombination in post-irradiation thymocytes. The 0w-10w above the figures indicates thymocytes 0–10 weeks after irradiation. Clonality is shown below the figures as partial clones (P), oligo-clones (O) and mono-clones (M). (**C**) Appearance of clones after irradiation. Open squares, open circles and closed circles indicate partial clones, oligo-clones plus mono-clones and total clones, respectively. (**D**) Examples of *TCRβ* recombination profiles in thymocytes and their derived thymic lymphomas (TL). Interstitial bands between germline and D2/J2.1 bands in 6w-8 lymphomas and those between D2/J2.3 and D2/J2.5 in 8w-14 and 10w-3 thymocytes are artificial hybrid bands produced by PCR. Clonality is shown below the figure. In (**B**) and (**D**), recombination profiles between D1 and J2.6 are not shown.

8w-14 and 9 of 10 cells in 8w-17, while the frequency was low in thymocyte populations bearing partial clones or non-clones, e.g. 2 of 34 cells in 10w-7 and 1 of 35 cells in 10w-1, suggesting that the clones themselves were prelymphoma cells.

Most of the thymic lymphomas bore *Notch1* rearrangements, but the rearranged sequences differed among the resultant lymphomas and from those in thymocytes (see Supplementary Tables 4 and 6). Thus, *Notch1* was rearranged after intrathymic injection of thymocytes, i.e. after prelymphoma cells were established.

DISCUSSION

The findings of the present study indicated that radiation caused thymic atrophy, and delayed induction of ROS, DNA lesions, chromosomal instability and bystander effects; as well as the generation of prelymphoma cells in intrathymic immature T cells of C57BL mice during radiation-induced thymic lymphomagenesis. Although bystander effects were not known to occur *in vivo* in the present study, other effects representing the intrinsic *in vivo* characteristics of post-irradiation immature T cells were induced *in vivo*. The delayed occurrence of these phenomena indicates that the events were not induced by direct radiation effects, but rather by indirect radiation effects, suggesting the involvement of microenvironmental changes, e.g. thymic atrophy. Microenvironmental changes generate inflammatory conditions [4, 5]. Radiation-induced thymic atrophy, a characteristic condition leading to thymic lymphomagenesis [11, 12], is thought to produce an inflammatory condition, including production of ROS in the thymus by redox-mediating enzymes activated during inflammation [25, 45]. Thus, the nontargeted effects described

here might reflect inflammatory-type responses to radiation-induced stress and injury [14, 28].

Increased ROS in immature T cells are thought to induce DNA damage. The occurrence of the nontargeted effects coincides with the stage of ROS induction, suggesting that intracellular and extracellular ROS are primary causes of these nontargeted effects. The following findings support this notion: (i) H_2O_2 induced aneuploidy and chromosomal aberrations in thymocytes; (ii) bystander effects of thymocytes were observed in co-cultured, ROS-sensitive mutant cells; and (iii) treatment of thymocytes with catalase and SOD abolished the bystander effects. Therefore, our scenario of radiation induction of thymic lymphomas is that radiation causes microenvironmental changes, such as thymic atrophy. The change might induce inflammatory conditions leading to ROS production, which results in the induction of nontargeted effects, such as chromosomal instability and bystander effects. Delayed chromosomal instability induces aneuploidy and karyotypic changes in immature T cells. Immature T cells with an altered karyotype expand clonally and eventually become prelymphoma clones that convert to overt thymic lymphomas after activation of the oncogene *Notch1* by rearrangement. Thus, chromosomal instability drives radiation-induced thymic lymphomagenesis through the induction of characteristic changes of immature T cells and the generation of prelymphoma cells, consistent with reports that increased ROS cause thymic lymphomas by inducing chromosomal instability in $Atm^{-/-}$ [46] and $p53^{-/-}$ mice [47]. If the chromosomal instability is caused by ROS or their reacted products, it would be due to either ROS produced by the cells themselves or bystander effects through ROS or ROS-reacted products produced by the surrounding cells.

How do ROS induce chromosomal instability? 8-Oxoguanine is a major oxidative base lesion in DNA or nucleotides. 8-Oxoguanine accumulates in the nuclear DNA and mitochondrial DNA of $Ogg1^{-/-}$ cells exposed to ROS-generating agents and single-strand DNA breaks are generated during S phase through the MUTYH function [34]. Our data indicate that chromosomal aberrations are induced in $Ogg1^{-/-}$ cells by co-culture with post-irradiation immature T cells. These findings suggest that ROS in post-irradiation immature T cells promote the generation of 8-oxoguanine in either the nucleotide pool or DNA, thereby increasing the accumulation of 8-oxoguanine in DNA during replication, which in turn leads to the accumulation of single-strand breaks or even double-strand breaks. In this scenario, radiation-induced ROS are expected to cause chromosomal instability through the accumulation of 8-oxoguanine in DNA. Increased ROS cause the accumulation of 8-oxoguanine in DNA and induce mutation [47]. Preliminary measurement of 8-oxoguanine in DNA based on the binding of avidin with 8-oxoguanine in DNA [48] indicated significant accumulations of 8-oxoguanine in post-irradiation thymocytes 13 weeks after irradiation (unpublished data). Detailed analyses of the presence of 8-oxoguanine in DNA post-irradiation are needed.

Aneuploidy is a predisposing factor for carcinogenesis [20, 21]. Defects in the mitotic spindle checkpoint and sister-chromatid separation pathway or formation of the anaphase bridge result in high chromosome loss rates and aneuploidy [21, 49]. Aneuploidy might be induced by radiation-induced ROS through the above two pathways, because ROS, on the one hand, decrease activity in anaphase promoting complexes [50] to ubiquitinate securin, which induces a lagging chromatid due to incorrect microtubule-kinetochore attachment, and, on the other hand, cause chromatid exchanges leading to anaphase bridges in thymocytes (as revealed by the induction of chromatid exchanges 6 to 10 weeks after irradiation; see Supplementary Table 3). Because mis-segregation of chromosomes in mitosis occurs randomly [51], the increase in trisomy 15-bearing cells after irradiation is due to selective expansion after generation. Comparison of phenotypes between injected thymocytes and resulting thymic lymphomas indicated that the acquisition of trisomy 15 is an important step in lymphomagenesis; that is, the establishment of prelymphoma cells and development of thymic lymphomas, although there are also various minor pathways. In contrast to the role of aneuploidy in solid tumours, in which several chromosomes participate in aneuploidy and karyotypic imbalance is involved [52], the role of aneuploidy of the specific chromosome in lymphomagenesis is probably due to specific genes located on the chromosome, i.e. the *Myc* gene [12].

Abolishment of bystander effects in mutant cells co-cultured with T cell-depleting thymocytes indicates that the main effectors are immature T cells. This does not exclude the possibility that activated macrophages and neutrophils function in the bystander effect by interacting with immature T cells. These cells observed in inflammatory conditions are likely sources of bystander signals [16, 19, 28]. It is not known whether increased ROS are due to alterations of immature T cells or an interaction between immature T cells and surrounding cells.

Although the present study suggests ROS induction by indirect radiation effects, direct effects cannot be excluded because the mice received whole-body irradiation. To distinguish these effects, we transplanted nonirradiated wild-type thymuses into irradiated scid mice and measured ROS levels in transplanted thymuses. Thymic hypoplasia, ROS induction and lymphoma development sequentially occurred in transplanted thymuses (unpublished data), indicating that ROS induction in nonirradiated thymocytes is due to an indirect effect of radiation.

Characterization of prelymphoma cells will contribute to a better understanding of the process of radiation-induced thymic lymphomagenesis. The abnormal characteristics of

TL2-positive prelymphoma cells, such as aneuploidy or karyotypic changes, are not known [30, 31]. Although immature T cell clones with identical *TCRβ* rearrangements are suspected prelymphoma cells [12, 29], this has not been confirmed. We show that these clones bearing an altered karyotype are prelymphoma cells. Because even cells without *TCRβ* rearrangements become prelymphoma cells, the *TCRβ* rearrangements themselves might not elicit neoplastic potential. Instead, they might be a hallmark of expanded prelymphoma clones. We could not examine their phenotypes in detail because of difficulties in isolating them. The ability to isolate prelymphoma cells using an adequate marker is needed to characterize these cells in further detail.

ACKNOWLEDGEMENTS

This work was supported by grants for the Research Program of the Radiation Effect Mechanisms of the National Institute of Radiological Sciences. We thank Taeko Iwai and Tomoko Kawasaki for excellent animal care.

SUPPLEMENTARY MATERIAL

Supplementary material is available at the *Journal of Radiation Research* online.

REFERENCES

1. Kaplan HS, Brown MB. A quantitative dose-response study of lymphoid-tumor development in irradiated C57 black mice. *J Natl Cancer Inst* 1952;**13**:185–208.
2. Wright EG, Cortes PJ. Untargeted effects of ionizing radiation: implications for radiation pathology. *Mutat Res* 2006;**597**:119–32.
3. Wright EG. Manifestations and mechanisms of non-targeted effects of ionizing radiation. *Mutat Res* 2010;**687**:28–33.
4. Barcellos-Hoff MH, Nguyen DH. Radiation carcinogenesis in context: how do irradiated tissues become tumors? *Health Phys* 2009;**97**:446–57.
5. Barcelloss-Hoff MH, Park C, Wright EG. Radiation and the microenvironment—tumorigenesis and therapy. *Nat Rev Cancer* 2005;**5**:867–75.
6. Kaplan HS, Hirsh BB, Brown MB. Indirect induction of lymphomas in irradiated mice. IV. Genetic evidence of the origin of the tumor cells from the thymic grafts. *Cancer Res* 1956;**16**:434–6.
7. Muto M, Sado T, Hayata I *et al*. Reconfirmation of indirect induction of radiogenic lymphomas using thymectomized, irradiated B10 mice grafted with neonatal thymuses from Thy 1 congenic donors. *Cancer Res* 1983;**43**:3822–7.
8. Dührsen U, Metcalf D. Effects of irradiation of recipient mice on the behavior and leukemogenic potential of factor-dependent hematopoietic cell lines. *Blood* 1990;**75**:190–7.
9. Barcellos-Hoff MH, Ravani SA. Irradiated mammary gland stroma promotes the expression of tumorigenic potential by unirradiated epithelial cells. *Cancer Res* 2000;**60**:1254–60.
10. Morgan JE, Gross JG, Pagel CN *et al*. Myogenic cell proliferation and generation of a reversible tumorigenic phenotype are triggered by preirradiation of the recipient site. *J Cell Biol* 2002; **157**:693–702.
11. Sado T, Kamisaku H, Kubo E. Bone marrow-thymus interaction during thymic lymphomagenesis induced by fractionated radiation exposure in B10 mice: analysis using bone marrow transplantation between Thy 1 congenic mice. *J Radiat Res* 1991;**32** (Suppl 2):168–80.
12. Ohi H, Mishima Y, Kamimura K *et al*. Multi-step lymphomagenesis deduced from DNA changes in thymic lymphomas and atrophic thymuses at various times after gamma-irradiation. *Oncogene* 2007;**26**:5280–9.
13. Kaplan HS, Brown MB, Paull J. Influence of bone-marrow injections on involution and neoplasia of mouse thymus after systemic irradiation. *J Natl Cancer Inst* 1953;**14**:303–16.
14. Lorimore SA, Coates PJ, Wright EG. Radiation-induced genomic instability and bystander effects: inter-related nontargeted effects of exposure to ionizing radiation. *Oncogene* 2003;**22**:7058–69.
15. Azzam EI, de Toledo SM, Little JB. Oxidative metabolism, gap junctions and the ionizing radiation-induced bystander effect. *Oncogene* 2003;**22**:7050–7.
16. Watson GE, Lorimore SA, Macdonald DA *et al*. Chromosomal instability in unirradiated cells induced in vivo by a bystander effect of ionizing radiation. *Cancer Res* 2000;**60**:5609–11.
17. Watson GE, Pocock DA, Papworth D *et al*. In vivo chromosomal instability and transmissible aberrations in the progeny of haemopoietic stem cells induced by high- and low-LET radiation. *Int J Radiat Biol* 2001;**77**:409–17.
18. Gowans ID, Lorimore SA, Mcllrath JM *et al*. Genotype-dependent induction of transmissible chromosomal instability by gamma-radiation and the benzene metabolite hydroquinone. *Cancer Res* 2005;**65**:3527–30.
19. Lorimore SA, Chrystal JA, Robinson JI *et al*. Chromosomal instability in unirradiated hemopoietic cells induced by macrophages exposed *in vivo* to ionizing radiation. *Cancer Res* 2008;**68**:8122–6.
20. Lengauer C, Kinzler KW, Vogelstein B. Genetic instabilities in human cancer. *Nature* 1998;**396**:643–9.
21. Holland AJ, Cleveland DW. Boveri revisited: chromosomal instability, aneuploidy and tumorigenesis. *Nat Rev Mol Cell Biol* 2009;**10**:478–87.
22. Ponnaiya B, Cornforth MN, Ullrich RL. Radiation-induced chromosomal instability in BALB/c and C57BL/6 mice: the difference is as clear as black and white. *Radiat Res* 1997;**147**:121–5.
23. Ullrich RL, Ponnaiya B. Radiation-induced instability and its relation to radiation carcinogenesis. *Int J Radiat Biol* 1998;**74**:747–54.
24. Boulton E, Cleary H, Papworth D *et al*. Susceptibility to radiation-induced leukaemia/lymphoma is genetically separable from sensitivity to radiation-induced genomic instability. *Int J Radiat Biol* 2001;**77**:21–9.

25. Zhao W, Diz DI, Robbins ME. Oxidative damage pathways in relation to normal tissue injury. *Brit J Radiol* 2007;**80**:523–31.
26. Coates PJ, Lorimore SA, Wright EG. Damaging and protective cell signalling in the untargeted effects of ionizing radiation. *Mutat Res* 2004;**568**:5–20.
27. Narayanan PK, Goodwin EH, Lehnert BE. Alpha particles initiate biological production of superoxide anions and hydrogen peroxide in human cells. *Cancer Res* 1997;**57**: 3963–71.
28. Lorimore SA, Coates PJ, Scobie GE *et al*. Inflammatory-type responses after exposure to ionizing radiation in vivo: a mechanism for radiation-induced bystander effects? *Oncogene* 2001;**20**:7085–95.
29. Suzuki G, Shimada Y, Hayashi T *et al*. An association between oxidative stress and radiation-induced lymphomagenesis. *Radiat Res* 2004;**161**:642–7.
30. Muto M, Kubo E, Sado T. Development of prelymphoma cells committed to thymic lymphomas during radiation-induced thymic lymphomagenesis in B10 mice. *Cancer Res* 1987;**47**:3469–72.
31. Muto M, Kubo E, Kamisaku H *et al*. Phenotypic characterization of thymic prelymphoma cells of B10 mice treated with split-dose irradiation. *J Immunol* 1990;**144**:849–53.
32. Boyer JC, Umar A, Risinger JI *et al*. Microsatellite instability, mismatch repair deficiency, and genetic defects in human cancer cell lines. *Cancer Res* 1995;**55**:6063–70.
33. Katsube T, Mori M, Tsuji H *et al*. Differences in sensitivity to DNA-damaging agents between *XRCC4*- and *Artemis*-deficient human cells. *J Radiat Res* 2011;**52**:415–24.
34. Oka S, Ohno M, Tsuchimoto D *et al*. Two distinct pathways of cell death triggered by oxidative damage to nuclear and mitochondrial DNAs. *EMBO J* 2008;**27**:421–32.
35. Yoshimura D, Sakumi K, Ohno M *et al*. An oxidized purine nucleoside triphosphatase, MTH1, suppresses cell death caused by oxidative stress. *J Biol Chem* 2003;**278**:37965–73.
36. Sakamoto K, Tominaga Y, Yamauchi K *et al*. MUTHY-null mice are susceptible to spontaneous and oxidative stress-induced intestinal tumorigenesis. *Cancer Res* 2007;**67**:6599–604.
37. Ushijima Y, Tominaga Y, Miura T *et al*. A functional analysis of the DNA glycosylase activity of mouse MUTYH protein excising 2-hydroxyadenine opposite guanine in DNA. *Nucleic Acids Res* 2005;**33**:672–82.
38. Chen T, Kubo E, Sado T *et al*. Cytogenetic analysis of thymocytes during early stages after irradiation in mice with different susceptibilities to radiation-induced lymphomagenesis. *J Radiat Res* 1996;**37**:267–76.
39. ISCN. An International System for Human Cytogenetic Nomenclature, Mitelman F (ed). S. Kargar: Basel, 1995.
40. Tsuji H, Ishii-Ohba H, Katsube T *et al*. Involvement of illegitimate V(D)J recombination or microhomology-mediated nonhomologous end-joining in the formation of intragenic deletions of the *Notch1* gene in mouse thymic lymphomas. *Cancer Res* 2004;**64**:8882–90.
41. Tsuji H, Ishii-Ohba H, Noda Y *et al*. Rag-dependent and Rag-independent mechanisms of *Notch1* rearrangement in thymic lymphomas of $Atm^{-/-}$ and scid mice. *Mutat Res* 2009;**660**:22–32.
42. Kawamoto H, Ohmura K, Fujimoto S *et al*. Extensive proliferation of T cell lineage-restricted progenitors in the thymus: an essential process for clonal expression of diverse T cell receptor beta chains. *Eur J Immunol* 2003;**33**:606–15.
43. Emerit I, Cerutti PA. Tumor promoter phorbol-12-myristate-13-acetate induces chromosomal damage via indirect action. *Nature* 1981;**293**:144–6.
44. Tsuji H, Ishii-Ohba H, Ukai H *et al*. Radiation-induced deletions in the 5'-end region of *Notch1* lead to the formation of truncated proteins and are involved in the development of mouse thymic lymphomas. *Carcinogenesis* 2003;**24**:1257–68.
45. Novo E, Parola M. Redox mechanisms in hepatic wound healing and fibrogenesis. *Fibrogenesis Tissue Repair* 2008;**1**:5–63.
46. Ito K, Takubo K, Arai F *et al*. Regulation of reactive oxygen species by *Atm* is essential for proper response to DNA double-strand breaks in lymphocytes. *J Immunol* 2007;**178**:103–10.
47. Sablina AA, Budanov AV, Ilyinskaya GV *et al*. The antioxidant function of the p53 tumor suppressor. *Nat Med* 2005;**12**:1306–13.
48. Struthers L, Patel R, Clark J *et al*. Direct detection of 8-oxodeoxyguanosine and 8-oxoguanine by avidin and its analogues. *Anal Biochem* 1998;**255**:20–31.
49. Stewenius Y, Gorunova L, Jonson T *et al*. Structural and numerical chromosome changes in colon cancer develop through telomere-mediated anaphase bridges, not through mitotic multipolarity. *Proc Natl Acad Sci USA* 2005; **102**:5541–6
50. Chang T-S, Jeong W, Lee D-Y *et al*. The ring-H2 – finger protein APC11 as a target of hydrogen peroxide. *Free Radic Biol Med* 2004;**37**:521–30.
51. Torosantucci L, De Santis Puzzonia M, Cenciarelli C *et al*. Aneuploidy in mitosis of PtK1 cells is generated by random loss and nondisjunction of individual chromosomes. *J Cell Sci* 2009;**122**:3455–61.
52. Nicholson JM, Duesberg P. On the karyotypic origin and evolution of cancer cells. *Cancer Genet Cytogenet* 2009;**194**:90–110.